

On the Convergence of Multicalibration Gradient Boosting

Daniel Haimovich¹ Fridolin Linder¹ Lorenzo Perini¹ Niek Tax¹ Milan Vojnović^{1,2}

Abstract

Multicalibration gradient boosting has recently emerged as a scalable method that empirically produces approximately multicalibrated predictors and has been deployed at web scale. Despite this empirical success, its convergence properties are not well understood. In this paper, we bridge the gap by providing convergence guarantees for multicalibration gradient boosting in regression with squared-error loss. We show that the magnitude of successive prediction updates decays at $O(1/\sqrt{T})$, which implies the same convergence rate bound for the multicalibration error over rounds. Under additional smoothness assumptions on the weak learners, this rate improves to linear convergence. We further analyze adaptive variants, showing local quadratic convergence of the training loss, and we study rescaling schemes that preserve convergence. Experiments on real-world datasets support our theory and clarify the regimes in which the method achieves fast convergence and strong multicalibration.

1. Introduction

Multicalibration has emerged as a rigorous criterion for trustworthy machine learning, requiring predictions to match true outcome expectations not only globally, but across a virtually unlimited class of (potentially overlapping) subpopulations (Hebert-Johnson et al., 2018; Haghtalab et al., 2023; Pfisterer et al., 2021). While originally applied for algorithmic fairness, multicalibration has proven relevant for general model reliability, improving (1) robustness against distribution shifts (Kim et al., 2022; Wu et al., 2024) and (2) performance in downstream tasks ranging from ranking to uncertainty quantification (Yang et al., 2024; Detommaso et al., 2024; Dwork et al., 2022).

¹Meta, London, United Kingdom ²LSE, Department of Statistics, London, United Kingdom. Contact: Daniel Haimovich <danielha@meta.com>, Fridolin Linder <flinder@meta.com>, Lorenzo Perini <lorenzoperini@meta.com>, Niek Tax <niek@meta.com>, Milan Vojnović <m.vojnovic@lse.ac.uk>.

To achieve this in practice, a new class of *multicalibration gradient boosting* methods has recently been developed (Tax et al., 2026; Jin et al., 2025). Unlike traditional post-processing methods that rely on grid discretization, these algorithms iteratively refine a predictor by training an ensemble of weak learners on residuals, dynamically augmenting the feature space at each round with the predictions from the previous round. Such an approach has shown significant empirical success: it requires no manual group specification, scales to large datasets and, as highlighted by MCGRAD (Tax et al., 2026), can be deployed in production environments at web scale.

Despite this empirical adoption, the theory that supports multicalibration gradient boosting methods remains underexplored. These algorithms induce a dynamic optimization problem: because the predictions at the t -th iteration become a feature input for round $t+1$, the optimization target shifts at every iteration, making existing convergence proofs for standard gradient boosting invalid for this setting. Thus, fundamental questions remain unanswered: does the sequence of predictors actually converge to a multicalibrated predictor? How fast do they converge to a multicalibrated predictor? Can we guarantee stability when rescaling updates to prevent overfitting? Without theoretical guarantees, practitioners must rely solely on heuristics, which might be risky for safety-critical applications.

In this paper, we bridge the gap between empirical success and theoretical guarantees. We introduce a convergence analysis of multicalibration gradient boosting in the regression setting with squared-error loss. Defining the empirical multicalibration error as the correlation between a predictor’s residuals and the functions in the weak learner hypothesis class, we show that this error is bounded by the magnitude of the update step—the gap between successive predictions. By modeling the algorithm as an evolving system, we analyze the convergence of this gap to zero, which implies multicalibration.

Our main contributions can be summarized as follows:

- **Convergence and Rate:** We prove that for the standard algorithm, the gap between successive prediction values converges to zero with a decay rate of $O(1/\sqrt{T})$, where T is the number of rounds. Furthermore, un-

der smoothness assumptions on the weak learners, we show a linear convergence rate (i.e., the error decreases by a constant factor $0 < \kappa < 1$ per round).

- **Guarantees for Rescaling Variants:** We extend our analysis to practical variants used to mitigate overfitting. We show that the $O(1/\sqrt{T})$ rate holds even when using relaxed rescaling weights (i.e., converging to 1 asymptotically).
- **Convergence with Adaptive Weights:** We analyze an adaptive variant where rescaling weights are optimized at each step to minimize training loss. We prove that this method converges to a multicalibrated limit point and, provided the initial error is sufficiently small, the training loss converges to zero at a quadratic rate.
- **Empirical Validation:** We support our theoretical findings with experiments on real-world datasets, showing that the gap between prediction values indeed decreases with a geometric rate.

By proving these results, we provide the first theoretical justification for the stability and efficiency of iterative multicalibration gradient boosting, which plays a fundamental role for its continued deployment in real-world systems.

2. Related Work

Foundations of Multicalibration. Hebert-Johnson et al. (2018) introduced multicalibration, showing that a predictor can be calibrated across a potentially exponential family of intersecting subpopulations using an iterative postprocessing algorithm (HKRR). Dwork et al. (2021) later unified this line of work under *outcome indistinguishability*, placing multicalibration as a relaxation of indistinguishability from the true distribution. Related notions include *multiaccuracy* (Kim et al., 2019) and *low-degree multicalibration* (Gopalan et al., 2022b), which weaken calibration constraints to low-degree polynomial moments.

Subsequent work suggested that multicalibration does not need to arise solely from post-hoc correction, but can instead emerge as a natural fixed point of empirical risk minimization (ERM). Gopalan et al. (2022a) introduced *omniprediction*, showing that multicalibrated predictors support optimal decision-making across a broad class of convex loss functions (Hu et al., 2023). Building on this perspective, Globus-Harris et al. (2023) established an equivalence between multicalibration and Bayes optimality under a swap-regret condition, leading to *swap-agnostic learning* (Gopalan et al., 2023). Globus-Harris et al. (2023) further connected multicalibration to boosting for squared-error regression through repeated calls to weak learners for squared error regression on subsets of the data distribution.

Multicalibration via Gradient Boosting. Motivated by these connections, recent work has explored achieving multicalibration directly within gradient boosting. These approaches fit residuals using ensembles of decision trees, where each boosting round is defined with respect to the predictor from the previous round. A key feature is that trees are trained on an extended input space that augments the original features with the current prediction. Jin et al. (2025) proposed such a method and showed that approximate multicalibration can be achieved in a single round under a *loss saturation condition*, which requires that further rounds yield only marginal improvement. Similarly, Tax et al. (2026) introduced MCGRAD, a recursive GBDT method deployed at web-scale. They showed that the multicalibration error can be bounded by a function of the gap between successive predictions, but did not establish that this gap converges to zero.

Despite strong empirical performance, existing gradient boosting approaches lack convergence guarantees for arbitrarily many rounds. Current guarantees either rely on single-round analysis under a loss saturation condition (Jin et al., 2025) or assume diminishing gaps between successive predictions (Tax et al., 2026). In contrast, we study the *finite-time dynamics* of multi-round boosting and derive convergence and rate guarantees.

Extensions Beyond the Mean. Although our analysis focuses on mean multicalibration, prior work has extended calibration guarantees to higher-order properties. The *HappyMap* framework (Deng et al., 2023) generalizes calibration targets to arbitrary statistics (e.g., quantiles), while Jung et al. (2021) introduced *moment multicalibration* to control variance. Gupta et al. (2022) and Jung et al. (2023) further developed *multivalidity* for constructing prediction intervals, primarily in online learning settings. Our results complement these advances by providing the first rigorous convergence rates for the batch boosting dynamics underlying practical multicalibration methods.

Proof Techniques. Our analysis builds on matrix algebra constructs similar to those used in (Lu and Mazumder, 2020), but applies them to a distinct multi-round boosting procedure with dynamically evolving features. While rescaling predictions has been used in regression to improve generalization (Xu et al., 2017), our work differs in its focus on ensembles of weak learners operating on feature representations that evolve across boosting rounds.

3. Preliminaries and Problem Setup

Multicalibration and Notation. We consider a regression setting with data points $(x_1, y_1), \dots, (x_n, y_n) \in \mathbb{R}^d \times \mathbb{R}$, assumed to be i.i.d. from a distribution D . We denote

the vector of targets as $y = (y_1, \dots, y_n)^\top$ and a predictor as $f: \mathbb{R}^{d \times n} \rightarrow \mathbb{R}^n$. We will intentionally use the same notation f to indicate the map and the prediction vector $f(x_1, \dots, x_n)$.

Let \mathcal{B} be a finite set of functions (weak learners), where $b_j: \mathbb{R}^d \times \mathbb{R} \rightarrow \mathbb{R}$ for each $b_j \in \mathcal{B}$. The cardinality of \mathcal{B} is denoted by p . A key feature of multicalibration boosting methods is that predictors interact with other predictions: intuitively, $b_j(x, f)$ represents a predicted response for a given feature vector x and an auxiliary prediction feature f . For any prediction vector $f \in \mathbb{R}^n$ (where f_i corresponds to x_i), we define the matrix-valued function $B(f) \in \mathbb{R}^{n \times p}$ such that the j -th column is $(b_j(x_1, f_1), \dots, b_j(x_n, f_n))^\top$.

Note that the set of weak learners can be arbitrarily large but finite. This assumption allows analysis in a finite-dimensional space and covers common weak learners such as regression trees and parametric models with floating-point parameters.

The multicalibration errors of a predictor f with respect to the hypothesis class of functions \mathcal{B} are defined as the vector $\mathcal{E}(f) \in \mathbb{R}^p$ with components

$$\epsilon_j = \mathbb{E}_{(x,y) \sim D}[(y - f(x))b_j(x, f(x))]$$

for $j = 1, \dots, p$. The predictor f is *multicalibrated* with respect to the hypothesis class \mathcal{B} if $\mathcal{E}(f) = 0$. This can be extended naturally to the relaxed notion of α -multicalibration, which requires $\|\mathcal{E}(f)\| \leq \alpha$ for some norm function $\|\cdot\|$. The multicalibration error can also be seen as the correlation between the residuals and the weak learners evaluated at the current predictions. Similarly, the empirical multicalibration errors are defined as the sample means over the given dataset:

$$\widehat{\mathcal{E}}(f) := \frac{1}{n}B(f)^\top(y - f). \quad (1)$$

Factorised Hypothesis Classes. A special type of the set \mathcal{B} consists of functions that admit the following factorisation. Let $\mathcal{H} = \{h: \mathbb{R}^d \rightarrow \mathbb{R}\}$ and $\mathcal{G} = \{g: \mathbb{R} \rightarrow \mathbb{R}\}$ be finite sets of functions with cardinalities m and k , respectively. For every $b \in \mathcal{B}$, we have $b(x, u) = h(x)g(u)$ for some $g \in \mathcal{G}$ and $h \in \mathcal{H}$. For this type of function, the matrix $B(f)$ can be expressed as follows. Let $h(x) = (h_1(x), \dots, h_m(x))^\top$ and $g(u) = (g_1(u), \dots, g_k(u))^\top$. Then define

$$b(x, u) = h(x) \otimes g(u) \in \mathbb{R}^p \quad (2)$$

where \otimes denotes the Kronecker product¹ and $p = mk$, and let

$$B(f) = (b(x_1, f_1), \dots, b(x_n, f_n))^\top. \quad (3)$$

¹For any two vectors $u \in \mathbb{R}^m$ and $v \in \mathbb{R}^k$, $u \otimes v = (u_1 v^\top, \dots, u_m v^\top)^\top \in \mathbb{R}^{mk}$.

Algorithm 1 Multicalibration Gradient Boosting

Input: Initial predictor f_0 , data (X, y) , step size $\eta \in (0, 1]$, number of rounds $T > 0$.

for $t = 0, \dots, T - 1$ **do**

1. Compute the matrix $B(f_t)$ using the current predictions f_t .
2. Fit ensemble θ_t to residuals: $\theta_t \approx \arg \min_{\theta} \|y - f_t - B(f_t)\theta\|_2^2$.
3. Update: $f_{t+1} = w_t(f_t + \eta B(f_t)\theta_t)$.

end for

The Multicalibration Boosting Framework. We analyze the class of *multicalibration gradient boosting* algorithms (Tax et al., 2026; Jin et al., 2025). Unlike standard boosting, these methods dynamically update the feature space at every round by including the model’s current prediction. The procedure is formalized in Algorithm 1: at round t , the algorithm fits an ensemble of weak learners to the residuals $y - f_t$, using the features augmented by f_t .

The candidate predictor at round t is rescaled by a weight w_t to obtain the predictor for round $t+1$. By default $w_t = 1$ (no rescaling). We also consider relaxed rescaling weights following a fixed schedule and adaptive rescaling weights depending on prediction values; see Section 4.3 for details.

We analyze the algorithm in the limit where the weak learner ensemble perfectly approximate the projection of the residuals onto the span of \mathcal{B} . This induces the following *discrete-time dynamical system*:

$$f_{t+1} = w_t(f_t + \eta A(f_t)(y - f_t)), \quad (4)$$

where $A(f) := B(f)B(f)^\top$ is the orthogonal projector onto the column space of $B(f)$, and $B(f)^\top$ denotes the Moore-Penrose inverse of $B(f)$. The term $A(f_t)(y - f_t)$ represents the best approximation of the residuals using the hypothesis class \mathcal{B} conditioned on the current predictions.

Crucially, the empirical multicalibration error is bounded by the update step size. In fact, from Eq. (1) and (4), for unit weights ($w_t = 1$), we have:

$$\|\widehat{\mathcal{E}}(f_t)\|_2 \leq \frac{1}{n\eta} \|B(f_t)\|_2 \|f_{t+1} - f_t\|_2. \quad (5)$$

Thus, under assumption that $\{\|B(f_t)\|_2\}$ is uniformly bounded, showing that the *gap* $\|f_{t+1} - f_t\|_2$ converges to zero is sufficient to prove asymptotic multicalibration. Moreover, a convergence rate bound holding for the prediction gap implies the same convergence rate bound for multicalibration (up to a constant factor).

We admit a regularity condition that $b_j(x, f)$ functions are such that for every (x, f) in a compact set, $b_j(x, f)$ have a bounded range. This ensures that $\{\|B(f_t)\|_2\}$ is uniformly

bounded provided that $\{\|f_t\|_2\}$ is uniformly bounded. The latter condition is shown to hold for the multicalibration gradient boosting algorithms studied in the paper.

4. Main Results

In this section, we present our main theoretical contributions. First, we show the fundamental convergence of the dynamical system (Eq. (4)), proving that the empirical multicalibration error goes to 0 with a $O(1/\sqrt{T})$ rate. Second, we investigate the conditions that allow for faster (linear) rates. Finally, we extend these guarantees to algorithmic variants that are more likely to be deployed in real-world systems (adaptive rescaling).

Assumption: Employing a Boosting Oracle. Our analysis relies on an assumption regarding the gradient boosting step. In each round t , the boosting machine outputs a linear combination of weak learners $B(f_t)\theta_t$, where $B(f) \in \mathbb{R}^{n \times p}$ is the matrix of weak learner evaluations defined in Eq. (3). We assume the booster is run for sufficient iterations to effectively compute the *optimal* coefficient vector $\theta_t \in \mathbb{R}^p$ that minimizes the squared error loss:²

$$\theta_t := \arg \min_{\theta \in \mathbb{R}^p} \frac{1}{2} \|y - f_t - B(f_t)\theta\|_2^2.$$

Geometrically, this implies that the update direction is the orthogonal projection of the residuals onto the subspace spanned by the current weak learners. This assumption allows us to model the algorithm as the deterministic dynamical system defined in Eq. (4). This assumption is justified by fast convergence of gradient boosting machines; e.g., in (Lu and Mazumder, 2020), it was shown that, under suitable conditions, gradient boosted machines converge exponentially fast for any smooth, strongly-convex loss function. In Section 5, we present numerical results obtained using gradient boosting regression with a finite number of iterations per round, which validate our theoretical results.

4.1. Fundamental Convergence Guarantees

Our key result shows that the multicalibration gradient boosting dynamic is stable: the residuals are non-increasing, and the system converges to multicalibrated limit points.

Theorem 4.1 (Convergence with No Rescaling). *Consider the dynamical system in Eq. (4) with constant unit rescaling weights ($w_t = 1$). Then:*

1. **Non-increasing Loss:** *The loss is non-increasing: $\|y - f_{t+1}\|_2 \leq \|y - f_t\|_2$.*

²If $B(f_t)$ is not full column rank, we assume that θ_t is the minimum-norm minimiser of the squared error loss.

2. **Asymptotic Multicalibration:** *The gap between successive predictions satisfies $\|f_{t+1} - f_t\|_2 \rightarrow 0$, implying diminishing multicalibration error.*

3. **Convergence Rate:** *The minimum gap between successive predictions decays as*

$$\min_{0 \leq t \leq T-1} \|f_{t+1} - f_t\|_2 \leq \frac{\sqrt{\eta}\|y - f_0\|_2}{\sqrt{T}}.$$

Sketch. The result relies on the Lyapunov function method, with the Lyapunov function equal to the squared norm of the residuals (up to a constant factor). The increments of this Lyapunov function are non-positive and proportional to the squared norm of the gap between successive predictions between rounds. The sum of these differences over T steps is bounded by the initial error $\|y - f_0\|^2$. This implies that the squared error gaps must converge to 0 with a rate of $O(1/T)$, yielding the $O(1/\sqrt{T})$ rate for the gap itself. See Appendix A.1 for the full proof. \square

This theorem provides the first theoretical justification for the success of boosting algorithms like MCGRAD (Tax et al., 2026). It guarantees that, despite the changing feature space, the algorithm converges to a limit set of points and effectively minimizes the multicalibration error.

4.2. When is Convergence Fast?

While Theorem 4.1 guarantees sublinear convergence, empirical insights (see Section 5) often suggest faster (linear) convergence. Therefore, we investigate the structural properties of the hypothesis class \mathcal{B} required to allow such faster convergence rates.

Theorem 4.2 (Linear Convergence under Smoothness). *Assume $A(f)$ is Lipschitz continuous with constant L_A along the trajectory $\{f_t\}$ and let $\kappa := 1 - \eta + \eta L_A \|y - f_0\|_2$. Then, for every $t \geq 1$:*

$$\|f_{t+1} - f_t\|_2 \leq \kappa \|f_t - f_{t-1}\|_2.$$

As a result, if $\kappa < 1$, then the gap converges to zero linearly (geometrically fast).

Sketch. Using the update rule and the Lipschitz property of $A(f)$, we can bound the perturbation of the update step. Specifically, $\|A(f_t) - A(f_{t-1})\| \leq L_A \|f_t - f_{t-1}\|$. By substituting this into the recursive definition of the error, we derive the κ . Provided that the product of the smoothness constant L_A and the norm of the initial residual is small enough to keep $\kappa < 1$, the map acts as a contraction. See Appendix A.2 for the full proof. \square

The Lipschitz continuity of the projector $A(f)$ is a non-trivial condition. It holds for smooth weak learners under some spectral properties of matrix $B(f)$ as shown next.

Lemma 4.3 (Smoothness of $A(f)$). *Assume that for some $\mathcal{F} \subseteq \mathbb{R}^n$, for every $f \in \mathcal{F}$, $B(f)$ is Lipschitz continuous with constant L_B , $B(f)$ has the smallest singular value at least $\delta > 0$, and $\|B(f)\|_2 \leq M$, for some $M > 0$. Then, $A(f)$ is Lipschitz continuous on \mathcal{F} with constant:*

$$L_A \leq \frac{2}{\delta} \left(1 + c \frac{M^2}{\delta^2} \right) L_B$$

where $c = (1 + \sqrt{5})/2$.

Sketch. The result relies on the perturbation theory of Moore-Penrose pseudoinverses. Writing $A(f) = B(f)B(f)^+$, we decompose the difference $\|A(u) - A(v)\|_2$ into terms involving $B(u) - B(v)$ and $B(u)^+ - B(v)^+$. Using standard perturbation bounds (Stewart, 1977), the Lipschitz constant of $B(f)^+$ is bounded by terms involving the inverse of the smallest singular value δ . Combining these yields the bound on L_A . See Appendix A.3 for details. \square

For the factorized functions common in multicalibration (defined in Section 3), we can explicitly bound the Lipschitz constant L_B .

Lemma 4.4 (Smoothness of $B(f)$ for Factorized Learners). *Let \mathcal{B} consist of factorized functions $b(x, u) = h(x)g(u)$. If every $g \in \mathcal{G}$ is L_G -Lipschitz, then $A(f)$ is Lipschitz. Specifically, the Lipschitz constant L_B satisfies:*

$$L_B \leq (\max_i \|h(x_i)\|_2) \sqrt{k} L_G.$$

Sketch. For factorized functions, the evaluation matrix $B(f)$ admits a decomposition that completely splits the fixed features vectors $h(x_i)$ from the prediction-dependent terms $g(u)$. Because the feature vectors remain constant throughout the process, the sensitivity of $B(f)$ to changes in f is determined solely by the smoothness of g , scaled by the magnitude of the features. Consequently, the Lipschitz constant L_B is bounded by the product of the maximum feature norm $\max_i \|h(x_i)\|_2$ and the internal Lipschitz constant L_G . See Appendix A.4 for the full derivation. \square

This lemma links the abstract stability of the algorithm to the concrete smoothness of the weak learners ($g(u)$) and the diversity of the features ($H(X)$). This aligns with the intuition that “sharp” variations in weak learner behavior (e.g., unstable decision tree splits) might harm fast convergence.

4.3. Relaxed and Adaptive Rescaling Strategies

In practice, the simple additive updates ($w_t = 1$) can lead to overfitting. Practitioners often employ some rescaling of w_t to regularize the predictor. Here, we show that our convergence guarantees are robust to such modifications.

Relaxed Rescaling. We first consider the case where the weights $w_t \in (0, 1]$ approach 1 asymptotically.

Theorem 4.5 (Convergence with Relaxed Weights). *Assume that rescaling weights $\{w_t\}$ satisfy $\sum(1 - w_t) < \infty$. Then, (1) the training loss converges to a limit point, (2) the asymptotic multicalibration and (3) the $O(1/\sqrt{T})$ convergence rate of the gap $\|f_{t+1} - f_t\|_2$ established in Theorem 4.1 still hold. Specifically, the following holds:*

$$\min_{0 \leq t \leq T-1} \|f_{t+1} - f_t\|_2 \leq \frac{\sqrt{\eta}\|y - f_0\|_2 + \gamma}{\sqrt{T}}$$

where γ is a constant depending on η, y, f_0 and $\sum(1 - w_t)$.

Sketch. We modify the Lyapunov analysis from Theorem 4.1. With weights $w_t \in [0, 1]$, the decrease in the Lyapunov function is perturbed by an error ξ_t proportional to $(1 - w_t)$. The condition $\sum(1 - w_t) < \infty$ ensures these perturbations are summable, meaning the total “drift” away from the standard trajectory is bounded. This allows us to bound the accumulated error γ and preserve the $O(1/\sqrt{T})$ convergence rate. See Appendix A.5 for the full proof. \square

The result of the theorem confirms that relaxing the weights for regularization does not break the convergence results. The key assumption for the result in Theorem 4.5 to hold is that the sequence $\{w_t\}$ has sufficiently fast asymptotic convergence to 1, i.e., the condition $\sum(1 - w_t) < \infty$ holds.

The non-increasing loss property of Theorem 4.1 is not guaranteed to hold in the relaxed case. However, the following property can be shown to hold:

$$\|y - f_t\|_2 \leq \rho_t \|y - f_0\|_2 + (1 - \rho_t) \|y\|_2$$

where $\rho_t = \prod_{s=0}^{t-1} w_s$. This recovers the non-increasing training loss property in the case of unit rescaling weights, in which case $\rho_t \equiv 1$. In general, the gap between the training loss at round t and the initial training loss is guaranteed to be at most $(\|y\|_2 - \|y - f_0\|_2)(1 - \rho_t)$, which converges to a limit point – close to 0 if the rescaling weights converge sufficiently fast.

In the convergence rate bound, the constant γ is increasing in $\sum(1 - w_t)$. It achieves value 0 when $\sum(1 - w_t) = 0$, i.e., for unit-valued rescaling weights. In this case, the bound coincides to that of Theorem 4.1.

Adaptive Rescaling. A more aggressive strategy is to optimize w_t at each step. We define the adaptive weight $\omega(f_t)$ as the minimizer of $\|y - \omega\varphi(f_t)\|_2$, where $\varphi(f_t) = f_t + \eta A(f_t)(y - f_t)$ is the unscaled update direction. This yields the closed form

$$\omega(f_t) = \frac{y^\top \varphi(f_t)}{\|\varphi(f_t)\|_2^2}. \quad (6)$$

Table 1. Statistics of the datasets including the count of raw features, the total dimensionality (d) after pre-processing, the dataset size (n).

Dataset	Number of Raw Features	Total Number of Features	Number of Data Points
California Housing	8	8	20640
Diabetes	10	10	442
Adult	13	101	26048
German Credit	10	48	1000
Communities and Crime	122	122	1595

This transforms the system into $f_{t+1} = \omega(f_t)\varphi(f_t)$, effectively projecting y onto the 1D subspace of the current update.

The following result shows that monotonicity and asymptotic multicalibration remain to hold by using adaptive rescaling weights instead of unit-valued rescaling weights.

Theorem 4.6 (Convergence with Adaptive Rescaling). *Assume that the rescaling weights are adaptive according to Eq. (6). Then, (1) the non-increasing property of the loss and (2) the asymptotic multicalibration established in Theorem 4.1 still hold. In addition, (3) the rescaling weights are such that $\omega(f_t) \geq 0$, i.e., the angle between y and $\varphi(f_t)$ is acute or right (they point generally in the same direction).*

Sketch. Monotonicity holds because the adaptive step $\omega(f_t)$ explicitly minimizes the residual norm along the update direction. Asymptotic multicalibration is shown via a compactness argument: the sequence is confined to a finite-dimensional subspace, and any limit point must satisfy the stationarity conditions of the optimization. Finally, the non-negative sign of the weights follows from analyzing the spectrum of the update operator, showing that the update vector $\varphi(f_t)$ always forms an acute (or right) angle with the target y . See Appendix A.6 for the full proof. \square

In the following theorem, we show a local convergence result for the training loss to zero at a quadratic rate.

Theorem 4.7 (Quadratic Convergence Rate). *For the adaptive rescaling variant with $\eta = 1$ and some constant C , if the initial residuals are sufficiently small, the residual norm converges to zero at a quadratic rate:*

$$\|y - f_{t+1}\|_2 \leq C\|y - f_t\|_2^2,$$

Sketch. We derive a recurrence relation for the residuals r_{t+1} as a function of r_t . By performing a Taylor expansion around $r = 0$, we observe that the zero-th and first-order terms vanish due to the specific choice of the optimal step size $\omega(f_t)$. Consequently, the dominant term in the residual update is of order $\|r_t\|_2^2$, implying that once the error is small, it decays quadratically (similar to Newton's method). See Appendix A.7 for the full proof. \square

This result highlights the power of adaptive rescaling: by solving a simple 1D line-search at each step (computationally cheap operation), the algorithm can achieve Newton-like convergence properties near the optimum.

5. Numerical Results

In this section, we provide empirical validation for the theoretical claims presented in Section 4. Since our main contribution is the convergence analysis of the multicalibration gradient boosting dynamics, our experiments focus on verifying these rates and generalization properties on real-world data. Specifically, we aim to answer the following research questions:

- **RQ1 - Convergence with Unit Weights:** Does the gap between successive predictions converge to zero, and does the empirical rate align with the theoretical bounds?
- **RQ2 - Convergence with Rescaling Strategies:** Do the Relaxed and Adaptive rescaling strategies maintain the monotonicity of the loss and ensure asymptotic multicalibration?
- **RQ3 - Generalization:** How do these guarantees translate to generalization on unseen test data?

5.1. Experimental Setup

Data and Hyperparameters. We evaluate the algorithms on five standard regression datasets summarized in Table 1; see Appendix B.1 for more details. For all experiments, we use a Random Forest regressor (100 trees, max depth 5) as the initial predictor f_0 . The weak learners used in the boosting steps are 100 regression trees (max depth 3), implemented via scikit-learn's gradient boosting (learning rate 0.1).

Rescaling. We consider three rescaling strategies: UNIT sets $w_t = 1$, RELAXED uses the power-law decay $w_t = 1 - (t + 2)^{-3}$, and ADAPTIVE optimizes the weights via Eq. (6) in each round. We run the algorithms for $T = 20$ rounds with shrinkage $\eta = 1$.

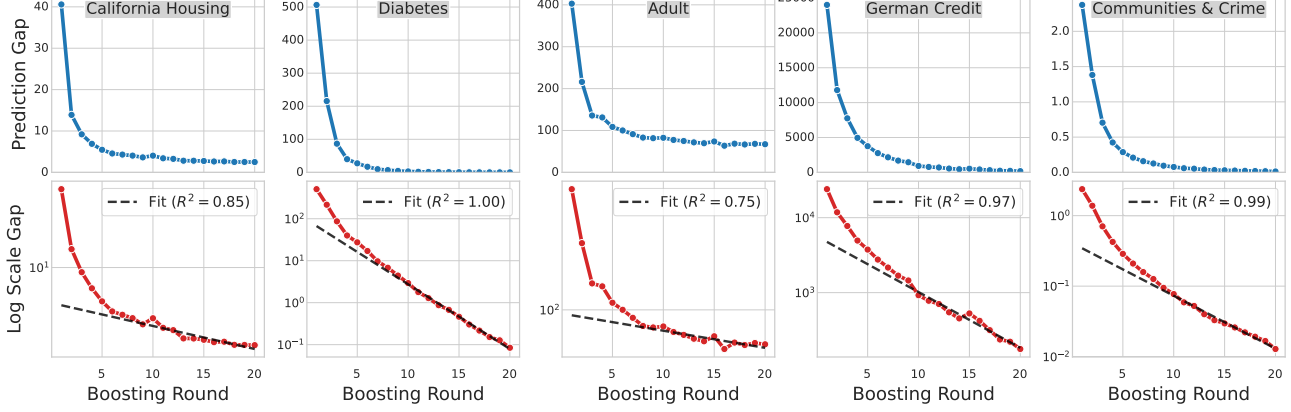


Figure 1. The prediction gap $\|f_{t+1} - f_t\|_2$ for all multicalibration boosting rounds $t \leq 20$. The bottom row shows the corresponding plots on a log-lin scale, along with the best fitting line (black) and its R^2 score.

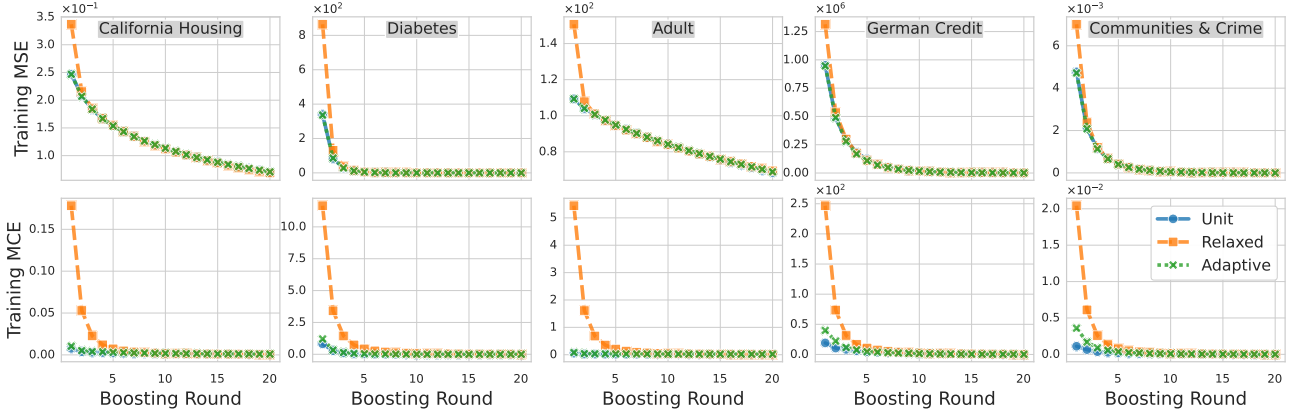


Figure 2. Evolution of the training MSE (top row) and training MCE (bottom row) over 20 boosting rounds across five datasets.

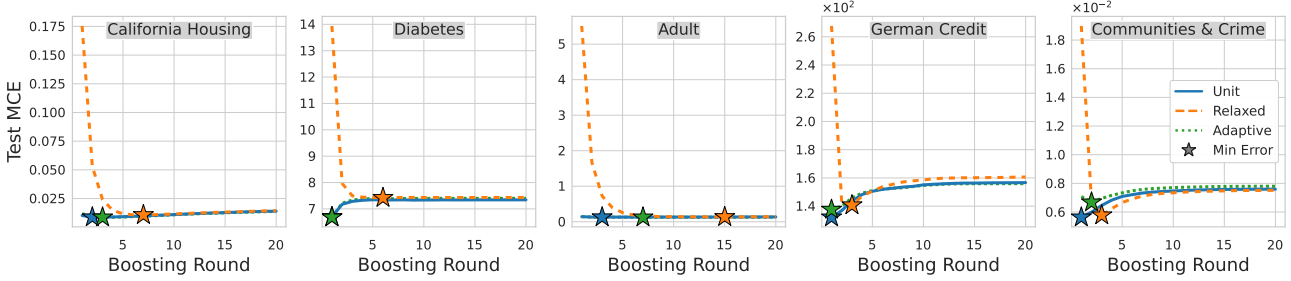


Figure 3. Average test Multicalibration Error (MCE) per dataset, with star markers indicating the optimal stopping point for each strategy.

5.2. Experimental Results

RQ1: Convergence with Unit Weights. Theorem 4.1 guarantees that the gap $\|f_{t+1} - f_t\|_2$ decays at a rate of at least $O(1/\sqrt{T})$. Furthermore, Theorem 4.2 establishes that under smoothness conditions on the weak learners, this rate improves to linear (geometric decay).

To validate these bounds, Figure 1 shows the evolution of the prediction gap from two perspectives. The top row displays the gap on a linear scale, showing a strict monotonic decay toward zero across all datasets, which empirically confirms the global convergence guarantees of Theorem 4.1.

To verify the stronger claim of linear convergence, the bot-

tom row shows the same values on a semi-log scale. In this view, a linear trajectory implies geometric decay (i.e., $\|f_{t+1} - f_t\|_2 \propto \kappa^t$ for some $\kappa < 1$). We fit a linear regression to the tail of the log-gap sequence (dashed black lines) and observe strictly linear behavior. The high R-squared values — ranging from 0.75 on Adult to 1.00 on Diabetes — provide empirical evidence that the convergence is indeed geometric. This supports the hypothesis that real-world ensembles of regression trees satisfy the smoothness conditions required for the faster rates derived in Theorem 4.2.

RQ2: Convergence with Rescaling Strategies. Theorems 4.5 and 4.6 guarantee that, over the rounds, (1) the training Mean Squared Error (MSE) is non-increasing and (2) the process achieves asymptotic multicalibration convergence. Thus, we investigate the reduction of the MSE and the Multicalibration Error (MCE) under the three considered rescaling strategies.

The top row of Figure 2 shows that every strategy yields a monotonic decrease in training MSE across all datasets. This confirms that the dynamic system remains stable regardless of the chosen rescaling. Interestingly, the **Relaxed** strategy (orange squares) shows a slightly slower initial convergence compared to **Unit** and **Adaptive** approaches; this is expected as the weights $w_t = 1 - (t+2)^{-3}$ are smaller in the early iterations, effectively harming the update step. On the other hand, the **Adaptive** strategy (green crosses) matches or exceeds the convergence speed of the unit baseline, showing that optimizing the rescaling weights w_t does not introduce instabilities.

While the MSE is a relevant loss, the main goal is to minimize the MCE. The bottom row of Figure 2 shows how the empirical MCE evolves over the rounds. Following our theoretical results, the plots show that the MCE has a consistent trend towards 0, often decreasing by some orders of magnitude (e.g., German Credit and Diabetes). The empirical results show a smooth and stable decay of multicalibration error to zero.

RQ3: Generalization. Finally, we examine how the theoretical convergence guarantees translate to unseen data. To make results more robust, we repeat the experiment for 20 different seeds and aggregate the test performance over the different runs. Figure 3 plots the average test MCE across iterations, with star markers indicating the optimal stopping point (minimum average error) for each strategy.

Unlike the monotonic trend of the training set (RQ2), the test error shows the classic bias-variance trade-off. In datasets such as *California Housing* and *German Credit*, we observe a distinct U-shaped evolution, where the error decreases initially before facing overfitting. This confirms that while the dynamical system is stable, regularization via early stopping

is necessary in practice.

Comparing the strategies shows a trade-off between efficiency and stability. The **Unit** and **Adaptive** strategies (blue and green lines) are highly efficient, typically reaching their optimal performance within the first 2-3 rounds. However, their aggressive updates can be harmful in some cases: this is most evident in the *German Credit* dataset, where they both overfit almost immediately. In contrast, the **Relaxed** strategy (orange dashed line) acts as an implicit regularizer. By reducing the early updates, it decays more gradually, shifting the optimal stopping point to later rounds (e.g., round 7 in *California Housing*). This makes the Relaxed strategy more robust to the choice of stopping time, reducing the risk of initial overfitting.

6. Conclusion

In this work, we have bridged the gap between the empirical success of multicalibration gradient boosting and its theoretical foundations. While algorithms like MCGRAD have been deployed at scale, their dynamic nature — where predictions recursively define the feature space — previously lacked rigorous analysis. By modeling this process as a deterministic dynamical system, we provided the first convergence guarantees for this class of algorithms in the regression setting.

Specifically, we proved that the gap between successive predictions converges to zero at a fundamental rate of $O(1/\sqrt{T})$, ensuring asymptotic multicalibration. We showed that under reasonable smoothness assumptions on the weak learners this rate improves to linear convergence, which is also supported by our empirical observation of geometric decay. Furthermore, we extended these guarantees to practical variants used in production. We showed that relaxed rescaling preserves the fundamental convergence rate while acting as an effective regularizer, and that adaptive rescaling can achieve quadratic convergence rates by optimizing the step size. Our experiments on real-world datasets validated these theoretical insights: the prediction gap decays geometrically, and the proposed rescaling strategies successfully mitigate overfitting.

Future Work. Our results open some future research directions. First, while our analysis focuses on the squared-error loss, extending these dynamical system arguments to general convex loss functions (e.g., logistic loss) is a natural next step. Second, our current model assumes a boosting oracle that solves the inner loop optimization; a finite-sample analysis that accounts for stochasticity and approximation errors in the weak learner training would further tighten the connection to practice. Finally, future work could leverage stability analysis to provide rigorous generalization error bounds for multicalibration boosting methods.

References

Zhun Deng, Cynthia Dwork, and Linjun Zhang. HappyMap : A Generalized Multicalibration Method. In Yael Tauman Kalai, editor, *14th Innovations in Theoretical Computer Science Conference (ITCS 2023)*, volume 251 of *Leibniz International Proceedings in Informatics (LIPIcs)*, pages 41:1–41:23, Dagstuhl, Germany, 2023. Schloss Dagstuhl – Leibniz-Zentrum für Informatik.

Gianluca Detommaso, Martin Bertran Lopez, Riccardo Fogliato, and Aaron Roth. Multicalibration for confidence scoring in LLMs. In *Forty-first International Conference on Machine Learning*, 2024.

Cynthia Dwork, Michael P Kim, Omer Reingold, Guy N Rothblum, and Gal Yona. Outcome indistinguishability. In *Proceedings of the 53rd Annual ACM SIGACT Symposium on Theory of Computing*, pages 1095–1108, 2021.

Cynthia Dwork, Michael P Kim, Omer Reingold, Guy N Rothblum, and Gal Yona. Beyond bernoulli: Generating random outcomes that cannot be distinguished from nature. In *International Conference on Algorithmic Learning Theory*, pages 342–380. PMLR, 2022.

Ira Globus-Harris, Declan Harrison, Michael Kearns, Aaron Roth, and Jessica Sorrell. Multicalibration as boosting for regression. In Andreas Krause, Emma Brunskill, Kyunghyun Cho, Barbara Engelhardt, Sivan Sabato, and Jonathan Scarlett, editors, *Proceedings of the 40th International Conference on Machine Learning*, volume 202 of *Proceedings of Machine Learning Research*, pages 11459–11492. PMLR, 23–29 Jul 2023.

Parikshit Gopalan, Adam Tauman Kalai, Omer Reingold, Vatsal Sharan, and Udi Wieder. Omnipredictors. In Mark Braverman, editor, *13th Innovations in Theoretical Computer Science Conference (ITCS 2022)*, volume 215 of *Leibniz International Proceedings in Informatics (LIPIcs)*, pages 79:1–79:21, Dagstuhl, Germany, 2022a. Schloss Dagstuhl – Leibniz-Zentrum für Informatik. ISBN 978-3-95977-217-4.

Parikshit Gopalan, Michael P. Kim, M. Singhal, and Shengjia Zhao. Low-degree multicalibration. In *Annual Conference Computational Learning Theory*, 2022b.

Parikshit Gopalan, Michael Kim, and Omer Reingold. Swap agnostic learning, or characterizing omniprediction via multicalibration. In A. Oh, T. Naumann, A. Globerson, K. Saenko, M. Hardt, and S. Levine, editors, *Advances in Neural Information Processing Systems*, volume 36, pages 39936–39956. Curran Associates, Inc., 2023.

Varun Gupta, Christopher Jung, Georgy Noarov, Mallesh M Pai, and Aaron Roth. Online multivalid learning: Means, moments, and prediction intervals. In *13th Innovations in Theoretical Computer Science Conference (ITCS 2022)*, pages 81:1–81:24, 2022.

Nika Haghtalab, Michael Jordan, and Eric Zhao. A unifying perspective on multi-calibration: Game dynamics for multi-objective learning. In *Thirty-seventh Conference on Neural Information Processing Systems*, 2023.

Ursula Hebert-Johnson, Michael Kim, Omer Reingold, and Guy Rothblum. Multicalibration: Calibration for the (Computationally-identifiable) masses. In Jennifer Dy and Andreas Krause, editors, *Proceedings of the 35th International Conference on Machine Learning*, volume 80 of *Proceedings of Machine Learning Research*, pages 1939–1948. PMLR, 10–15 Jul 2018.

Lunjia Hu, Inbal Rachel Livni Navon, Omer Reingold, and Chutong Yang. Omnipredictors for constrained optimization. In *International Conference on Machine Learning*, pages 13497–13527. PMLR, 2023.

Hongyi Henry Jin, Zijun Ding, Dung Daniel Ngo, and Steven Wu. Discretization-free multicalibration through loss minimization over tree ensembles. In *The Thirty-ninth Annual Conference on Neural Information Processing Systems*, 2025.

Christopher Jung, Changhwa Lee, Mallesh Pai, Aaron Roth, and Rakesh Vohra. Moment multicalibration for uncertainty estimation. In Mikhail Belkin and Samory Kpotufe, editors, *Proceedings of Thirty Fourth Conference on Learning Theory*, volume 134 of *Proceedings of Machine Learning Research*, pages 2634–2678. PMLR, 15–19 Aug 2021.

Christopher Jung, Georgy Noarov, Ramya Ramalingam, and Aaron Roth. Batch multivalid conformal prediction. In *The Eleventh International Conference on Learning Representations*, 2023.

Michael P Kim, Amirata Ghorbani, and James Zou. Multiaccuracy: Black-box post-processing for fairness in classification. In *Proceedings of the 2019 AAAI/ACM Conference on AI, Ethics, and Society*, pages 247–254, 2019.

Michael P Kim, Christoph Kern, Shafi Goldwasser, Frauke Kreuter, and Omer Reingold. Universal adaptability: Target-independent inference that competes with propensity scoring. *Proceedings of the National Academy of Sciences*, 119(4):e2108097119, 2022.

Haihao Lu and Rahul Mazumder. Randomized gradient boosting machine. *SIAM Journal on Optimization*, 30(4):2780–2808, 2020.

Florian Pfisterer, Christoph Kern, Susanne Dandl, Matthew Sun, Michael P. Kim, and Bernd Bischl. mcboost: Multicalibration boosting for r. *Journal of Open Source Software*, 6(64):3453, 2021.

G. W. Stewart. On the perturbation of pseudo-inverses, projections and linear least squares problems. *SIAM Review*, 19(4):634–662, 1977.

Niek Tax, Lorenzo Perini, Fridolin Linder, Daniel Haimovich, Dima Karamshuk, Nastaran Okati, Milan Vojnovic, and Pavlos Athanasios Apostolopoulos. MCGrad: Multicalibration at web scale. In *Proceedings of ACM KDD (Applied Data Science Track)*, 2026.

Jiayun Wu, Jiashuo Liu, Peng Cui, and Steven Z Wu. Bridging multicalibration and out-of-distribution generalization beyond covariate shift. *Advances in Neural Information Processing Systems*, 37:73036–73078, 2024.

Lin Xu, Shaobo Lin, Yao Wang, and Zongben Xu. Shrinkage degree in l_2 -rescale boosting for regression. *IEEE Transactions on Neural Networks and Learning Systems*, 28(8):1851–1864, 2017.

Shuai Yang, Hao Yang, Zhuang Zou, Linhe Xu, Shuo Yuan, and Yifan Zeng. Deep ensemble shape calibration: Multi-field post-hoc calibration in online advertising. In *Proceedings of the 30th ACM SIGKDD Conference on Knowledge Discovery and Data Mining*, pages 6117–6126, 2024.

A. Proofs and Additional Results

A.1. Proof of Theorem 4.1

We first note that $V(f) = \frac{1}{2}\|y - f\|_2^2$ is a Lyapunov function of the discrete-time dynamical system (4) that is nonincreasing along the trajectory $\{f_t\}$. To see this, note that

$$\begin{aligned} & V(f_{t+1}) - V(f_t) \\ &= \frac{1}{2}\|y - f_{t+1}\|_2^2 - \frac{1}{2}\|y - f_t\|_2^2 \\ &= -(y - f_t)^\top (f_{t+1} - f_t) + \frac{1}{2}\|f_{t+1} - f_t\|_2^2 \\ &= -(y - f_t)\eta A(f_t)(y - f_t) + \frac{1}{2}\eta^2\|A(f_t)(y - f_t)\|_2^2 \\ &= -\eta\left(1 - \frac{1}{2}\eta\right)\|A(f_t)(y - f_t)\|_2^2 \\ &= -\frac{1}{\eta}\left(1 - \frac{1}{2}\eta\right)\|f_{t+1} - f_t\|_2^2. \end{aligned}$$

From this we immediately observe that $V(f_{t+1}) - V(f_t) \leq 0$ for all $t \geq 0$, which is equivalent to nonincreasing residuals, i.e. $\|y - f_{t+1}\|_2 \leq \|y - f_t\|_2$, for all $t \geq 0$. This establishes the asserted non-increasing loss property.

As a side remark, note that $V(f_{t+1}) - V(f_t) < 0$ for every f_t that $A(f_t)(y - f_t) \neq 0$ and, otherwise, $V(f_{t+1}) - V(f_t) = 0$.

We next establish that $f_{t+1} - f_t$ is asymptotically regular, i.e., $\|f_{t+1} - f_t\|_2 \rightarrow 0$. For any $T \geq 0$,

$$V(f_T) - V(f_0) = -\frac{1}{\eta}\left(1 - \frac{1}{2}\eta\right)\sum_{t=0}^T\|f_{t+1} - f_t\|_2^2.$$

From this, it follows

$$\sum_{t=0}^{\infty}\|f_{t+1} - f_t\|_2^2 < \infty$$

which implies $\|f_{t+1} - f_t\|_2 \rightarrow 0$. This establishes that the gap between successive predictions converges to zero.

The convergence of the multicalibration error $\|\widehat{\mathcal{E}}(f_t)\|_2$ to zero can be established using Eq. (5) as follows. Since residuals $\|y - f_t\|_2$ are non-increasing, they are uniformly bounded. Combining with the fact $\|f_t\|_2 \leq \|y - f_t\|_2 + \|y\|_2$, we conclude that $\{\|f_t\|_2\}$ is uniformly bounded. From this, it follows that $\{\|B(f_t)\|_2\}$ is uniformly bounded. Therefore, using Eq. (5), there exists a constant $C > 0$ such that $\|\widehat{\mathcal{E}}(f_t)\|_2 \leq C\|f_{t+1} - f_t\|_2$. From this, it follows that $\|\widehat{\mathcal{E}}(f_t)\|_2 \rightarrow 0$, as we have already shown that $\|f_{t+1} - f_t\|_2 \rightarrow 0$.

Convergence Rate We have shown that, for all $t \geq 0$,

$$V(f_{t+1}) - V(f_t) = -\frac{1}{\eta}\left(1 - \frac{1}{2}\eta\right)\|f_{t+1} - f_t\|_2^2.$$

From this we have that, for all $t \geq 0$,

$$\|f_{t+1} - f_t\|_2^2 \leq 2\eta(V(f_t) - V(f_{t+1})).$$

Hence, we have

$$\begin{aligned} \sum_{t=0}^{T-1}\|f_{t+1} - f_t\|_2^2 &\leq 2\eta(V(f_0) - V(f_T)) \\ &\leq \eta\|y - f_0\|_2^2. \end{aligned}$$

From this, we conclude

$$\min_{0 \leq t \leq T-1}\|f_{t+1} - f_t\|_2 \leq \sqrt{\eta}\|y - f_0\|_2 \frac{1}{\sqrt{T}}.$$

A.2. Proof of Theorem 4.2

We first recall that for all $t \geq 1$,

$$A(f_t)(y - \tilde{f}_{t+1}) = 0$$

where $\tilde{f}_{t+1} = f_t + A(f_t)(y - f_t)$. Because $f_{t+1} = f_t + \eta A(f_t)(y - f_t)$, it can be readily checked that

$$\eta A(f_t)(y - f_{t+1}) = (1 - \eta)(f_{t+1} - f_t). \quad (7)$$

For all $t \geq 1$, we have

$$\begin{aligned}
& f_{t+1} - f_t \\
&= \eta A(f_t)(y - f_t) \\
&= \eta(A(f_t) - A(f_{t-1}))(y - f_t) + \eta A(f_{t-1})(y - f_t) \\
&= \eta(A(f_t) - A(f_{t-1}))(y - f_t) + (1 - \eta)(f_t - f_{t-1}) \\
&= \eta(A(f_t) - A(f_{t-1}))(I - \eta A(f_{t-1}))(y - f_{t-1}) \\
&\quad + (1 - \eta)(f_t - f_{t-1})
\end{aligned}$$

where the first and fourth equations hold by the definition of recurrence, and in the third equation we use Eq. (7).

It follows that

$$\|f_{t+1} - f_t\|_2 \leq (1 - \eta + \eta L_A \|y - f_0\|_2) \|f_t - f_{t-1}\|_2$$

which holds by the multiplicative norm inequality, the assumption that $A(f)$ is Lipschitz continuous with constant L_A , $\|I - \eta A(f)\|_2 \leq 1$, and $\|y - f_t\|_2$ is nonincreasing.

A.3. Proof of Lemma 4.3

Lemma A.1. *Assume that for some $u, v \in \mathbb{R}^n$, $B(u)$ and $B(v)$ have smallest singular values are at least $\delta > 0$ and for some $M > 0$, $\|B(u)\|_2, \|B(v)\|_2 \leq M$. Then,*

$$\|A(u) - A(v)\|_2 \leq \frac{2}{\delta} \left(1 + c \frac{M^2}{\delta^2}\right) \|B(u) - B(v)\|_2$$

where $c = (1 + \sqrt{5})/2$.

Proof. For any $f \in \mathbb{R}^n$, let $B_f \equiv B(f)$ and $A_f = B_f B_f^+$. Let u, v be two arbitrary vectors in \mathbb{R}^n . Assume that the smallest nonzero singular values of B_u and B_v are larger than or equal to $\delta > 0$. Moreover, assume that for some $M > 0$, $\|B_u\|_2 \leq M$ and $\|B_v\|_2 \leq M$.

By adding and subtracting terms, we have:

$$A_u - A_v = (B_u - B_v)B_u^+ + B_v(B_u^+ - B_v^+).$$

By the properties of the Moore-Penrose inverse, $B^+ = (B^\top B)^+ B^\top$. Using this, we have:

$$B_u^+ - B_v^+ = (B_u^\top B_u)^+ B_u^\top - (B_v^\top B_v)^+ B_v^\top.$$

By adding and subtracting terms, it holds:

$$\begin{aligned}
B_u^+ - B_v^+ &= ((B_u^\top B_u)^+ - (B_v^\top B_v)^+) B_u^\top \\
&\quad + (B_v^\top B_v)^+ (B_u - B_v)^\top.
\end{aligned}$$

Using the fact $(B^+)^T = B(B^\top B)^+$, we have

$$\begin{aligned}
B_v(B_u^+ - B_v^+) &= B_v((B_u^\top B_u)^+ - (B_v^\top B_v)^+) B_u^\top \\
&\quad + (B_v^+)^T (B_u - B_v)^\top.
\end{aligned}$$

Hence, it follows that:

$$\begin{aligned}
A_u - A_v &= (B_u - B_v)B_u^+ \\
&\quad + B_v((B_u^\top B_u)^+ - (B_v^\top B_v)^+) B_u^\top \\
&\quad + (B_v^+)^T (B_u - B_v)^\top.
\end{aligned}$$

Since $\|B_u\|_2 \leq M$ and $\|B_v\|_2 \leq M$, and

$$\|(B_u - B_v)B_u^+\|_2 \leq \frac{1}{\delta} \|B_u - B_v\|_2,$$

$$\|(B_v^+)^T (B_u - B_v)^\top\|_2 \leq \frac{1}{\delta} \|B_u - B_v\|_2$$

we have:

$$\begin{aligned}
\|A_u - A_v\|_2 &\leq \frac{2}{\delta} \|B_u - B_v\|_2 \\
&\quad + M^2 \|(B_u^\top B_u)^+ - (B_v^\top B_v)^+\|_2.
\end{aligned}$$

Since $(B^\top B)^+ = B^+(B^+)^T$ and $(B^+)^T = (B^T)^+$, it follows that:

$$\begin{aligned}
& (B_u^\top B_u)^+ - (B_v^\top B_v)^+ \\
&= B_u^+(B_u^+ - B_v^+)^T + (B_u^+ - B_v^+)(B_v^+)^T.
\end{aligned}$$

Hence, we have

$$\|(B_u^\top B_u)^+ - (B_v^\top B_v)^+\|_2 \leq \frac{2}{\delta} \|B_u^+ - B_v^+\|_2$$

It follows that:

$$\|A_u - A_v\| \leq \frac{2}{\delta} (\|B_u - B_v\|_2 + M^2 \|B_u^+ - B_v^+\|_2).$$

By Theorem 3.3 in (Stewart, 1977), we have:

$$\|B_u^+ - B_v^+\|_2 \leq c \max\{\|B_u^+\|_2^2, \|B_v^+\|_2^2\} \|B_u - B_v\|_2$$

where $c = (1 + \sqrt{5})/2$. Hence, it follows

$$\|B_u^+ - B_v^+\|_2 \leq \frac{c}{\delta^2} \|B_u - B_v\|_2.$$

Putting the pieces together, we have:

$$\|A_u - A_v\|_2 \leq \frac{2}{\delta} \left(1 + \frac{cM^2}{\delta^2}\right) \|B_u - B_v\|_2.$$

□

A.4. Proof of Lemma 4.4

We consider the case where \mathcal{B} contains factorised functions, as defined in Section 3, so that $B(f)$ is given by (2) and (3).

Recall that $h(x) = (h_1(x), \dots, h_m(x))^\top$ and $g(u) = (g_1(u), \dots, g_k(u))^\top$, for $x \in \mathbb{R}^d$ and $u \in \mathbb{R}$.

Define

$$H(X) = (h(x_1), \dots, h(x_n))^\top \in \mathbb{R}^{n \times m}$$

and

$$G(f) = (g(f_1), \dots, g(f_n))^\top \in \mathbb{R}^{n \times k}.$$

We can express $B(f)$ as follows:

$$B(f) = D_g(f) (H(X) \otimes I_k)$$

where

$$D_g(f) = \text{block-diag}(g(f_1)^\top, \dots, g(f_n)^\top).$$

From this, we have

$$\|B(f)\|_2 \leq \|G(f)\|_{2,\infty} \|H(X)\|_2$$

where $\|G(f)\|_{2,\infty} = \max\{\|g(f_1)\|_2, \dots, \|g(f_n)\|_2\}$.

Let

$$R(f) = D_h(X) (G(f) \otimes I_m)$$

where

$$D_h(X) = \text{block-diag}(h(x_1)^\top, \dots, h(x_n)^\top).$$

Notice that

$$\|B(f)\|_2 = \|R(f)\|_2.$$

Hence, it follows that

$$\|B(f)\|_2 \leq \|H(X)\|_{2,\infty} \|G(f)\|_2.$$

It also holds, for every $f, f' \in \mathbb{R}^n$,

$$\|B(f) - B(f')\|_2 = \|R(f) - R(f')\|_2.$$

Combining with

$$R(f) - R(f') = D_h(X) ((G(f) - G(f')) \otimes I_m)$$

we have

$$\|B(f) - B(f')\|_2 \leq \|H(X)\|_{2,\infty} \|G(f) - G(f')\|_2.$$

For the set of functions \mathcal{G} , such that every $g \in \mathcal{G}$ is L_G -Lipschitz continuous, we have

$$\|G(f) - G(f')\|_2 \leq L_G \sqrt{k} \|f - f'\|_2.$$

This can be readily checked as follows:

$$\begin{aligned} \|G(f) - G(f')\|_2 &\leq \|G(f) - G(f')\|_F \\ &= \sqrt{\sum_{j=1}^k \sum_{i=1}^m (g_j(f_i) - g_j(f'_i))^2} \\ &\leq \sqrt{\sum_{j=1}^k \sum_{i=1}^m L_G^2 (f_i - f'_i)^2} \\ &= L_G \sqrt{k} \|f - f'\|_2. \end{aligned}$$

A.5. Proof of Theorem 4.5

From Eq. (4), it readily follows:

$$y - f_{t+1} = (1 - w_t)y + w_t(I - \eta A(f_t))(y - f_t). \quad (8)$$

We consider the Lyapunov function

$$V(f) = \frac{1}{2} \|y - f\|_2^2.$$

By simple calculus,

$$\begin{aligned} &V(f_{t+1}) - V(f_t) \\ &= -w_t^2 \eta \left(1 - \frac{1}{2}\eta\right) \|A(f_t)(y - f_t)\|_2^2 + \xi_t \end{aligned} \quad (9)$$

where

$$\begin{aligned} \xi_t &= -\frac{1}{2}(1 - w_t^2) \|y - f_t\|_2^2 + \frac{1}{2}(1 - w_t)^2 \|y\|_2^2 \\ &\quad + w_t(1 - w_t)y^\top(I - \eta A(f_t))(y - f_t). \end{aligned}$$

From Eq. (8), using the fact $\|I - \eta A(f_t)\|_2 \leq 1$, we have

$$\|y - f_{t+1}\|_2 \leq (1 - w_t) \|y\|_2 + w_t \|y - f_t\|_2.$$

Since $w_t \in [0, 1]$ for all $t \geq 0$, it follows that $\{\|y - f_t\|_2\}$ is uniformly bounded.

By the Cauchy-Schwartz inequality and the fact $\|I - \eta A(f_t)\|_2 \leq 1$, it follows

$$\|y^\top(I - \eta A(f_t))(y - f_t)\|_2 \leq \|y\|_2 \|y - f_t\|_2.$$

Combining this with $\{\|y - f_t\|_2\}$ being uniformly bounded, we conclude that $\{\|y^\top(I - \eta A(f_t))(y - f_t)\|_2\}$ is uniformly bounded.

It follows that there exists a constant $C \geq 0$ such that

$$|\xi_t| \leq C(1 - w_t), \text{ for all } t \geq 0.$$

Under assumption $\sum_{t=0}^{\infty} (1 - w_t) < \infty$, we have

$$\sum_{t=0}^{\infty} |\xi_t| < \infty.$$

From Eq. (9), for any $T \geq 1$,

$$\begin{aligned} V(f_T) &\leq V(f_0) \\ &\quad - \eta \left(1 - \frac{1}{2}\eta\right) \sum_{t=0}^{T-1} w_t^2 \|A(f_t)(y - f_t)\|_2^2 \\ &\quad + \sum_{t=0}^{T-1} |\xi_t|. \end{aligned}$$

Since $V(f_T) \geq 0$ and $\sum_{t=0}^{T-1} |\xi_t| < \infty$, it follows that

$$\sum_{t=0}^{T-1} w_t^2 \|A(f_t)(y - f_t)\|_2^2 < \infty.$$

From this and the fact $w_t \rightarrow 1$, it follows that $\|A(f_t)(y - f_t)\|_2 \rightarrow 0$, i.e., $A(f_t)(y - f_t) \rightarrow 0$.

From the above observations, it readily follows that $V(f_T)$ is bounded. This implies that $\{\|f_t\|_2\}$ is uniformly bounded.

Now, note

$$f_{t+1} - f_t = w_t \eta A(f_t)(y - f_t) - (1 - w_t) f_t.$$

Hence, we have

$$\|f_{t+1} - f_t\|_2 \leq w_t \eta \|A(f_t)(y - f_t)\|_2 + (1 - w_t) \|f_t\|_2.$$

We have shown that $A(f_t)(y - f_t) \rightarrow 0$. Since $\{\|f_t\|_2\}$ is uniformly bounded and $w_t \rightarrow 1$, $(1 - w_t) \|f_t\|_2 \rightarrow 0$. It follows that

$$f_{t+1} - f_t \rightarrow 0.$$

This establishes that the gap between successive predictions converges to zero.

We next show that $V(f_t)$ converges to a limit point V^* . Let $s < t$. Note that

$$\begin{aligned} & V(f_t) - V(f_s) \\ &= -\eta \left(1 - \frac{1}{2}\eta\right) \sum_{i=s}^{t-1} w_i^2 \|A(f_i)(y - f_i)\|_2^2 \\ &\quad + \sum_{i=s}^{t-1} \xi_i, \end{aligned}$$

Hence, it holds

$$\begin{aligned} & |V(f_t) - V(f_s)| \\ &\leq \eta \left(1 - \frac{1}{2}\eta\right) \sum_{i=s}^{t-1} w_i^2 \|A(f_i)(y - f_i)\|_2^2 \\ &\quad + \sum_{i=s}^{t-1} |\xi_i|. \end{aligned}$$

Because both $w_t^2 \|A(f_t)(y - f_t)\|_2$ and $\|\xi_t\|_2$ converge to zero, their tails go to zero. Hence, for every $\epsilon > 0$, there exists $T \geq 0$ such that for all $t > s \geq T$, $|V(f_t) - V(f_s)| \leq \epsilon$. Thus, $\{V(f_t)\}$ is a Cauchy sequence, which implies that $V(f_t)$ converges to some limit point V^* .

We next establish asymptotic multicalibration. The dynamical system (4) can be written as:

$$f_{t+1} = w_t(f_t + \eta B(f_t)\theta(f_t)) \quad (10)$$

where $\theta(f_t)$ minimizes

$$\mathcal{L}_t(\theta) = \frac{1}{2} \|y - f_t - B(f_t)\theta\|_2^2.$$

The minimizer $\theta(f_t)$ satisfies the first-order optimality condition $\nabla \mathcal{L}_t(\theta(f_t)) = -B(f_t)^\top (y - f_t - B(f_t)\theta(f_t)) = 0$, that is,

$$B(f_t)^\top (y - f_t - B(f_t)\theta(f_t)) = 0. \quad (11)$$

From (10) and (11), for any sequence of rescaling weights satisfying $0 < w_t \leq 1$, we have

$$\widehat{\mathcal{E}}(f_t) = \frac{1 - w_t}{\eta w_t n} B(f_t)^\top f_t + \frac{1}{\eta w_t n} B(f_t)^\top (f_{t+1} - f_t).$$

We have already established that $\{\|f_t\|_2\}$ and $\|B(f_t)\|_2$ are uniformly bounded. Hence, there exist positive constants C_1 and C_2 such that

$$\|\widehat{\mathcal{E}}(f_t)\| \leq C_1 \frac{1 - w_t}{w_t} + C_2 \frac{1}{w_t} \|f_{t+1} - f_t\|_2.$$

Since $(1 - w_t)/w_t \rightarrow 0$, $1/w_t \rightarrow 1$, and $\|f_{t+1} - f_t\|_2 \rightarrow 0$, it follows that $\|\widehat{\mathcal{E}}(f_t)\| \rightarrow 0$.

Convergence Rate We first note the following identity.

Lemma A.2. *The difference of the successive residual norms satisfies, for every $t \geq 0$,*

$$\begin{aligned} & \|y - f_t\|_2^2 - \|y - f_{t+1}\|_2^2 \\ &= w_t \eta (2 - w_t \eta) \|A(f_t)(y - f_t)\|_2^2 \\ &\quad + (1 - w_t)^2 \|f_t\|_2^2 - 2(1 - w_t) f_t^\top (y - f_{t+1}). \end{aligned}$$

Proof. From (4), we have:

$$y - f_{t+1} = (I - w_t \eta A(f_t))(y - f_t) + (1 - w_t) f_t.$$

From this, it follows

$$\begin{aligned} \|y - f_{t+1}\|_2^2 &= \|(I - w_t \eta A(f_t))(y - f_t)\|_2^2 \\ &\quad + 2(1 - w_t) f_t^\top (I - w_t \eta A(f_t))(y - f_t) \\ &\quad + (1 - w_t)^2 \|f_t\|_2^2. \end{aligned}$$

Note that:

$$\begin{aligned} & \|(I - w_t \eta A(f_t))(y - f_t)\|_2^2 \\ &= \|y - f_t\|_2^2 - 2w_t \eta \|A(f_t)(y - f_t)\|_2^2 \\ &\quad + w_t^2 \eta^2 \|A(f_t)(y - f_t)\|_2^2. \end{aligned}$$

Hence, we have

$$\begin{aligned}
& \|y - f_t\|_2^2 - \|y - f_{t+1}\|_2^2 \\
&= 2w_t\eta \left(1 - \frac{1}{2}w_t\eta\right) \|A(f_t)r_t\|_2^2 \\
&\quad - (1 - w_t)^2 \|f_t\|_2^2 \\
&\quad - 2(1 - w_t)f_t^\top (I - w_t\eta A(f_t))(y - f_t).
\end{aligned}$$

From (4),

$$(I - w_t\eta A(f_t))(y - f_t) = (y - f_{t+1}) - (1 - w_t)f_t$$

which plugged in the last identity for the difference of the squared residual norms yields the assertion of the lemma. \square

Let V_t be the Lyapunov function defined as:

$$V_t = \frac{1}{2}\|y - f_t\|_2^2 + \sum_{s=0}^{t-1} (1 - w_s)f_s^\top (y - f_{s+1}) + C$$

where C is a sufficiently large constant. This constant needs to ensure that V_t is nonnegative. In order to ensure this, it is sufficient that:

$$C = C_w\rho$$

where, recall,

$$C_w = \sum_{t=0}^{\infty} (1 - w_t),$$

and,

$$\rho = \max\{2\|y\|_2^2, (\|y\|_2 + \|y - f_0\|_2)\|y - f_0\|_2\}.$$

In order to show this, it suffices to show that:

$$\left| \sum_{s=0}^{t-1} (1 - w_s)f_s^\top (y - f_{s+1}) \right| \leq C.$$

This clearly holds if, for all $t \geq 0$,

$$|f_t^\top (y - f_{t+1})| \leq \rho. \quad (12)$$

We next show that this inequality holds for every $t \geq 0$. By Cauchy-Schwartz, and the triangle inequality, we have

$$|f_t^\top (y - f_{t+1})| \leq (\|y\|_2 + \|y - f_t\|_2)\|y - f_{t+1}\|_2. \quad (13)$$

From (4), for all $t \geq 0$,

$$y - f_{t+1} = w_t(I - \eta A(f_t))(y - f_t) + (1 - w_t)y.$$

By the triangle inequality, the multiplicative norm inequality and the fact $\|I - \eta A(f)\|_2 \leq 1$, we have

$$\|y - f_{t+1}\|_2 \leq w_t\|y - f_t\|_2 + (1 - w_t)\|y\|_2.$$

From this it follows:

$$\|y - f_t\|_2 \leq \tilde{w}_t\|y - f_0\|_2 + (1 - \tilde{w}_t)\|y\|_2$$

where $\tilde{w}_t := \prod_{s=0}^{t-1} w_s \in [0, 1]$. Hence, we have:

$$\|y - f_t\|_2 \leq \max\{\|y - f_0\|_2, \|y\|_2\}.$$

Combining this with (13), we obtain (12).

Using Lemma A.2, we have

$$\begin{aligned}
& V_t - V_{t+1} \\
&= w_t\eta \left(1 - \frac{1}{2}w_t\eta\right) \|A(f_t)(y - f_t)\|_2^2 \\
&\quad + \frac{1}{2}(1 - w_t)^2 \|f_t\|_2^2 \\
&\geq 0
\end{aligned}$$

which shows that V_t is nonincreasing along any trajectory.

For any two vector sequences $\{a_t\}$ and $\{b_t\}$, by Cauchy-Schwartz inequality,

$$\|a_t + b_t\|_2^2 \leq \|a_t\|_2^2 + 2\|a_t\|_2\|b_t\|_2 + \|b_t\|_2^2.$$

By another application of the Cauchy-Schwartz inequality, we have

$$\begin{aligned}
\sum_{t=0}^{T-1} \|a_t + b_t\|_2^2 &= \sum_{t=0}^{T-1} \|a_t\|_2^2 \\
&\quad + 2\sqrt{\sum_{t=0}^{T-1} \|a_t\|_2^2} \sqrt{\sum_{t=0}^{T-1} \|b_t\|_2^2} \\
&\quad + \sum_{t=0}^{T-1} \|b_t\|_2^2.
\end{aligned}$$

We apply this to

$$f_{t+1} - f_t = w_t\eta A(f_t)(y - f_t) - (1 - w_t)f_t,$$

with $a_t = w_t\eta A(f_t)(y - f_t)$ and $b_t = -(1 - w_t)f_t$.

Note that

$$\begin{aligned}
& \|a_t\|_2^2 \\
&= \frac{w_t\eta}{1 - w_t\eta/2} \left(V_t - V_{t+1} - \frac{1}{2}(1 - w_t)^2 \|f_t\|_2^2 \right) \\
&\leq 2\eta(V_t - V_{t+1}).
\end{aligned}$$

and

$$\|b_t\|_2^2 \leq \tilde{\rho}(1 - w_t)^2$$

where $\tilde{\rho} = \|y\|_2 + \max\{\|y - f_0\|_2, \|y\|_2\}$.

Furthermore, note:

$$\begin{aligned}\sum_{t=0}^{T-1} \|a_t\|_2^2 &\leq 2\eta V_0 \\ &= \eta \|y - f_0\|_2^2 + 2\eta C \\ &= \eta \|y - f_0\|_2^2 + 2\eta\rho C_w\end{aligned}$$

and

$$\begin{aligned}\sum_{t=0}^{T-1} \|b_t\|_2^2 &= \tilde{\rho} \sum_{t=0}^{T-1} (1 - w_t)^2 \\ &\leq \tilde{\rho} \sum_{t=0}^{\infty} (1 - w_t)^2 \\ &= \tilde{\rho} \tilde{C}_w.\end{aligned}$$

It follows,

$$\begin{aligned}\sum_{t=0}^{T-1} \|f_{t+1} - f_t\|_2^2 &\leq \eta \|y - f_0\|_2^2 + 2\eta\rho C_w \\ &\quad + 2\sqrt{\|y - f_0\|_2^2 + 2\eta\rho C_w} \sqrt{\tilde{\rho} \tilde{C}_w} \\ &\quad + \tilde{\rho} \tilde{C}_w \\ &:= K.\end{aligned}$$

From this, it follows that:

$$\min_{0 \leq t \leq T-1} \|f_{t+1} - f_t\|_2 \leq \sqrt{K} \frac{1}{\sqrt{T}}.$$

By subadditivity of the square-root function,

$$\sqrt{K} \leq \sqrt{\eta} \|y - f_0\|_2 + \gamma$$

where

$$\gamma^2 = 2\eta\rho C_w + 2\sqrt{\|y - f_0\|_2^2 + 2\eta\rho C_w} \sqrt{\tilde{\rho} \tilde{C}_w} + \tilde{\rho} \tilde{C}_w.$$

A.6. Proof of Theorem 4.6

Non-increasing Loss. By definition, $\varphi(f_t) = f_t + \eta A(f_t)(y - f_t) = f_t + \eta B(f_t)\theta(f_t)$, where $\theta(f_t)$ is the minimiser of $\mathcal{L}_t(\theta) = \frac{1}{2}\|y - f_t - B(f_t)\theta\|_2^2$ over $\theta \in \mathbb{R}^p$. Hence,

$$\|y - \varphi(f_t)\|_2 \leq \|y - f_t\|_2.$$

Now, it clearly holds

$$\min_{\omega} \|y - \omega\varphi(f_t)\|_2 \leq \|y - \varphi(f_t)\|_2.$$

and, by definition of $\omega(f_t)$, $\|y - \omega(f_t)\varphi(f_t)\|_2 = \min_{\omega} \|y - \omega\varphi(f_t)\|_2$. Since $f_{t+1} = \omega(f_t)\varphi(f_t)$, it follows that

$$\|y - f_{t+1}\|_2 \leq \|y - f_t\|_2.$$

Non-negative Rescaling. Consider any iteration t such that $\varphi(f_t) \neq 0$. Using the facts that $f_{t+1} = M(f_t)y$ and $M(f_t)$ is an orthogonal projection matrix, we have:

$$\begin{aligned}\|y - f_{t+1}\|_2^2 &= \|y\|_2^2 - y^\top f_{t+1} + \|f_{t+1}\|_2^2 \\ &= \|y\|_2^2 - 2y^\top M(f_t)y + \|M(f_t)y\|_2^2 \\ &= \|y\|_2^2 - 2\|M(f_t)y\|_2^2 + \|M(f_t)y\|_2^2 \\ &= \|y\|_2^2 - \|M(f_t)y\|_2^2.\end{aligned}$$

Since $M(f) = \tilde{\varphi}(f)\tilde{\varphi}(f)^\top$, it follows:

$$\|y - f_{t+1}\|_2^2 = \|y\|_2^2 - (y^\top \tilde{\varphi}(f_t))^2.$$

Since $\|y - f_t\|_2$ is nonincreasing, we have $|y^\top \tilde{\varphi}(f_t)|$ is nondecreasing. By the Cauchy-Schwartz inequality, $|y^\top \tilde{\varphi}(f_t)| \leq \|y\|_2$, hence, $|y^\top \tilde{\varphi}(f_t)|$ is bounded. It follows that $|y^\top \tilde{\varphi}(f_t)|$ converges to a limit point.

It remains to show that $y^\top \tilde{\varphi}(f_t) \geq 0$ for all $t \geq 1$.

By definition, $\varphi(f) = f + \eta A(f)(y - f)$. Hence,

$$y^\top \varphi(f_t) = y^\top f_t + y^\top \eta A(f_t)(y - f_t).$$

Since $f_t = M(f_{t-1})y$, we have

$$y^\top \varphi(f_t) = y^\top (\eta A(f_t) + (I - \eta A(f_t))M(f_{t-1}))y.$$

We will use the following lemma.

Lemma A.3. For any orthogonal projection matrix A and a rank 1 matrix $M = vv^\top$ with $\|v\| = 1$, the eigenvalues of

$$\eta A + (I - \eta A)M$$

are the value 1 with multiplicity 1, $\eta\|(I - A)v\|_2^2$ with multiplicity 1, η with multiplicity $\text{rank}(A)$, and the value 0 with multiplicity $n - 1 - \text{rank}(A)$.

By the lemma, $\eta A(f_t) + (I - \eta A(f_t))M(f_{t-1})$ is a positive semi-definite matrix. Hence,

$$y^\top (\eta A(f_t) + (I - \eta A(f_t))M(f_{t-1}))y \geq 0$$

from which it follows $y^\top \varphi(f_t) \geq 0$.

Asymptotic Multicalibration. Let

$$u = f_0 - \frac{y^\top f_0}{\|y\|^2} y$$

Note that y and u are orthogonal vectors.

Since $\varphi(f) = \eta A(f)y + (I - \eta A(f))f$, by induction, for all $t \geq 0$, $\varphi(f_t)$ lies in the span of the vectors y and u . Since $f_{t+1} = \omega(f_t)\varphi(f_t)$, where $\omega(f_t)$ is a scalar value, it follows that for all $t \geq 0$, f_t lies in the span of y and u .

We can write for every $t \geq 0$,

$$\varphi(f_t) = a_t y + b_t u, \quad a_t, b_t \in \mathbb{R}.$$

It indeed holds:

$$y^\top \varphi(f_t) = a_t \|y\|_2^2$$

and

$$\|\varphi(f_t)\|_2^2 = a_t^2 \|y\|_2^2 + b_t^2 \|u\|_2^2.$$

Because $y^\top \varphi(f_t) > 0$ by assumption, we have $a_t > 0$ and $\|\varphi(f_t)\|_2 > 0$.

Hence,

$$\omega(f_t) = \frac{a_t \|y\|_2^2}{a_t^2 \|y\|_2^2 + b_t^2 \|u\|_2^2}.$$

By the Cauchy-Schwartz inequality, $y^\top \varphi(f_t) \leq \|y\|_2 \|\varphi(f_t)\|_2$ so

$$\omega(f_t) \leq \frac{\|y\|_2}{\|\varphi(f_t)\|_2}.$$

Therefore, the sequence $\{\omega(f_t)\}$ is a bounded above and below. Also $\{\varphi(f_t)\}$ is bounded and lies in the finite-dimensional subspace spanned by y and u , hence, it lies in a compact set.

By compactness, we can choose a subsequence t_i such that $\lim_{i \rightarrow \infty} \varphi(f_{t_i}) = \varphi^*$ and $\lim_{i \rightarrow \infty} \omega(f_{t_i}) = \omega^*$. From $f_{t_i+1} = \omega(f_{t_i})\varphi(f_{t_i})$, we obtain $\lim_{i \rightarrow \infty} f_{t_i+1} = f^*$, where $f^* = \omega^* \varphi^*$.

Now, since $\varphi(f_{t_i+1}) = f_{t_i+1} + \eta A(f_{t_i+1})(y - f_{t_i+1})$, using continuity of $A(f)$, we conclude that

$$\varphi^* = f^* + \eta A^*(y - f^*)$$

where $A^* \equiv A(f^*)$.

Substituting $f^* = \omega^* \varphi^*$, we have

$$N \varphi^* = \eta A^* y. \quad (14)$$

where $N := (1 - \omega^*)I + \omega^* \eta A^*$.

There are two cases, either $\omega^* \neq 1$ or $\omega^* = 1$.

Case 1: $\omega^* \neq 1$. In this case N is invertible. Hence, from (14), $\varphi^* = N^{-1} \eta A^* y$. Since $NA^* = (1 - \omega^* + \eta \omega^*)A^*$, we have $A^* y = (1 - \omega^* + \eta \omega^*)N^{-1}A^* y$. It follows that

$$(1 - \omega^* + \eta \omega^*) \varphi^* = \eta A^* y.$$

Plugging this into the definition of $\omega(f)$, we obtain

$$\omega^* = \frac{y^\top \varphi^*}{\|\varphi^*\|_2^2} = \frac{y^\top A^* y}{\|A^* y\|_2^2} \frac{1 - \omega^* + \eta \omega^*}{\eta} = \frac{1 - \omega^* + \eta \omega^*}{\eta}$$

which is equivalent to $\omega^* = 1$, contradicting the case assumption $\omega^* \neq 1$.

Case 2: $\omega^* = 1$. In this case $N = \eta A^*$ and equation (14) becomes:

$$A^* \varphi^* = A^* y.$$

Since $f^* = \omega^* \varphi^*$ and $\omega^* = 1$, $f^* = \varphi^*$. It follows that $A^*(y - f^*) = 0$, which concludes consideration of Case 2.

From the cases we have shown that any subsequential limit (ω^*, φ^*) must satisfy $\omega^* = 1$ and $A(f^*)\varphi^* = A(f^*)y$, with $\varphi^* = f^*$. Hence, every convergent subsequence of $\{\omega(f_t)\}$ has the same limit 1. Because $\{\omega(f_t)\}$ is bounded every subsequence limit equals 1, the whole sequence converges to 1.

A.7. Proof of Theorem 4.7

We first establish the following lemma:

Lemma A.4. *The residuals evolve according to the following iterative equation:*

$$r_{t+1} = \frac{y^\top (A(f_t)r_t)}{\|y - (I - A(f_t))r_t\|_2^2} (I - A(f_t))r_t. \quad (15)$$

Proof. We have

$$r_{t+1} = \frac{y\varphi(f_t)^\top - y^\top \varphi(f_t)I}{\varphi(f_t)^\top \varphi(f_t)} \varphi(f_t).$$

For simplicity of notation, with a local scope to the proof of the lemma, we write φ and A in lieu of $\varphi(f)$ and $A(f)$. Note

$$\begin{aligned} & (y\varphi^\top - y^\top \varphi I)\varphi \\ &= (y\varphi^\top - y^\top \varphi I)(y + (I - A)(f - y)) \\ &= (y\varphi^\top - y^\top \varphi I)(I - A)(f - y), \end{aligned}$$

$$\begin{aligned} y\varphi^\top (I - A) &= y(f^\top + (y - f)^\top A)(I - A) \\ &= yf^\top (I - A) \end{aligned}$$

and

$$y^\top \varphi (I - A) = (y^\top f - y^\top A(f - y))(I - A).$$

Subtracting the last two identities, we have

$$(y\varphi^\top - y^\top \varphi I)(I - A) = y^\top A(f - y)(I - A).$$

Hence, it follows:

$$(y\varphi(f)^\top - y^\top \varphi I)\varphi = y^\top A(y - f)(I - A)(y - f).$$

Noting that $\varphi^\top \varphi = \|\varphi\|_2^2$ and $\varphi = y - (I - A)(y - f)$, we have

$$\varphi^\top \varphi = \|y - (I - A)(y - f)\|_2^2.$$

From the above relations, it follows that (15) holds. \square

By Lemma A.4, $r_{t+1} = g(r_t)/h(r_t)$, where

$$g(r) = (I - A(y - r))r (A(y - r)r)^\top y$$

and

$$h(r) = \|y - (I - A(y - r))r\|_2^2.$$

For small r , we have

$$g(r) = (I - A(y))r (A(y)r)^\top y + o(\|r\|_2^2).$$

From this, we observe that

$$\|g(r)\|_2 \leq \|y\|_2 \|r\|_2^2 + o(\|r\|_2^2).$$

For small r , we have

$$h(r) = \|y - (I - A(y))r\|_2^2 + o(\|r\|_2).$$

Assume that r is sufficiently small so that $h(r) \geq (1/2)\|y\|_2^2$. Then, we have

$$\left\| \frac{g(r)}{h(r)} \right\|_2 \leq \frac{2}{\|y\|_2} (1 + o(1)) \|r\|_2^2.$$

A.8. A Hybrid Boosting Algorithm

Here we consider an alternative boosting algorithm, defined by modifying the iterative update in Algorithm 1 as follows:

$$\hat{f}_{t+1}(x) = \hat{f}_t(x) + \eta[\delta\hat{f}_t(x) + \gamma(\hat{y}(x) - \hat{f}_t(x))]$$

where $\hat{y}(x)$ is some given predictor.

The key difference from our original algorithm is the additional term $\gamma(\hat{y}(x) - \hat{f}_t(x))$. Intuitively, we may regard this term as adding an extra predictor with a fixed weight γ , whose predictions are the approximate residuals $\hat{y}(x) - \hat{f}_t(x)$. If $\hat{y}(x)$ is a perfect predictor, then the extra predictor outputs are precisely the residuals $y(x) - \hat{f}_t(x)$. This extra predictor serves as a preconditioning to address the ill-conditioning of the matrix $A(f_t)$. The method can be considered as a hybrid boosting as we mix weak learners with a strong learner.

The dynamical system for f_t in the prevailing case can be expressed in the following form:

$$f_{t+1} = f_t - \eta[P(f_t)\nabla V(f_t) + \xi_t] \quad (16)$$

where $P(f_t) = \gamma I + A(f_t)$, $\xi_t = \gamma(y - \hat{y})$, and $V(f) = \frac{1}{2}\|y - f\|_2^2$. The iteration (16) is an inexact preconditioned gradient descent algorithm.

The multicalibration errors can be expressed as follows:

$$\widehat{\mathcal{E}}(f_t) = \gamma \frac{1}{n} B(f_t)^\top (y - \hat{y}) + \frac{1}{\eta n} B(f_t)^\top (f_{t+1} - f_t).$$

The following lemma provides a general convergence result for the inexact projected gradient descent algorithm in (16).

Lemma A.5. *Assume that $V : \mathbb{R}^n \rightarrow \mathbb{R}$ is a continuously differentiable function that is L -smooth and μ -strongly convex, $P(f)$ is a positive definite matrix such that for some constants $0 < m \leq M < \infty$, $mI \prec P(f) \prec M I$, and $(f - f^*)^\top P(f)\nabla V(f) \geq m(f - f^*)^\top \nabla V(f)$, where f^* is the minimiser of V . Then, for any step size $\eta \in (0, 2m\mu/(L^2M^2))$, the iterates satisfy:*

$$\|y - f_{t+1}\|_2 \leq \kappa \|y - f_t\|_2 + \eta \|\xi_t\|_2$$

where

$$\kappa = \sqrt{1 - 2\mu m \eta \left(1 - \frac{L^2 M^2}{\mu m} \eta\right)} < 1.$$

Proof is in Appendix A.9.

Applying Lemma A.5 to our boosting setting, we have the following convergence result:

Proposition A.6. *Assume that the shrinkage parameter satisfies $\eta \in (0, 2\gamma/(1 + \gamma)^2)$. Then, for all $t \geq 0$,*

$$\|y - f_{t+1}\|_2 \leq \kappa \|y - f_t\|_2 + \eta \gamma \|y - \hat{y}\|_2$$

where

$$\kappa = \sqrt{1 - 2\gamma \eta \left(1 - \frac{(1 + \gamma)^2}{\gamma} \eta\right)} < 1.$$

Proof is in Appendix A.10.

For the shrinkage parameter set as $\eta = c\gamma$, for some constant $0 < c < 1$, the condition on the shrinkage parameter is $\gamma < \sqrt{2/c} - 1$. For such a choice of the shrinkage parameter, $\kappa \approx 1 - 2c(1 - c)\gamma^2$ for small γ .

In general, we have:

$$\|y - f_t\|_2 \leq \kappa^t \|y - f_0\|_2 + \frac{\eta\gamma}{1 - \kappa} \|y - \hat{y}\|_2.$$

For the shrinkage parameter set as $\eta = c\gamma$, with $0 < c < 1$, we have: $\eta\gamma/(1 - \kappa) \approx (1 - c)/2$.

A.9. Proof of Lemma A.5

By the μ -strong convexity of V , for every f, f' ,

$$(f - f')^\top (\nabla V(f) - \nabla V(f')) \geq \mu \|f - f'\|_2^2,$$

and, by the L -smoothness of V , we have:

$$\|\nabla V(f) - \nabla V(f')\|_2 \leq L\|f - f'\|_2.$$

In particular, for every f , and f^* the minimiser of V , we have

$$(f - f^*)^\top \nabla V(f) \geq \mu\|f - f^*\|_2^2 \quad (17)$$

and

$$\|\nabla V(f)\|_2 \leq L\|f - f^*\|_2. \quad (18)$$

Let $\delta_t = f_t - f^* - \eta P(f_t) \nabla V(f_t)$. Note that

$$\begin{aligned} \|\delta_t\|_2^2 &= \|f_t - f^*\|_2^2 - 2\eta(f_t - f^*)^\top P(f_t) \nabla V(f_t) \\ &\quad + \eta^2 \|P(f_t) \nabla V(f_t)\|_2^2 \end{aligned}$$

By assumption, $(f - f^*)^\top P(f_t) \nabla V(f_t) \geq m(f_t - f^*)^\top \nabla V(f_t)$, which combined with (17) yields:

$$(f_t - f^*)^\top P(f_t) \nabla V(f_t) \geq m\mu\|f_t - f^*\|_2^2.$$

By assumption $P(f_t) \prec MI$, which combined with (18) yields:

$$\|P(f_t) \nabla V(f_t)\|_2 \leq ML\|f_t - f^*\|_2.$$

From the asserted relations it follows that:

$$\begin{aligned} \|\delta_t\|_2^2 &\leq \|f_t - f^*\|_2^2 - 2\eta m\mu\|f_t - f^*\|_2^2 \\ &\quad + \eta^2 M^2 L^2 \|f_t - f^*\|_2^2 \\ &= (1 - 2\eta m\mu + \eta^2 M^2 L^2) \|f_t - f^*\|_2^2. \end{aligned}$$

Hence, we have established that:

$$\|\delta_t\|_2^2 \leq \kappa^2 \|f_t - f^*\|_2^2$$

where

$$\kappa^2 = 1 - 2\eta m\mu + \eta^2 M^2 L^2.$$

To conclude the proof, note that:

$$\|f_{t+1} - f^*\|_2 = \|\delta_t - \eta \xi_t\|_2 \leq \|\delta_t\|_2 + \eta \|\xi_t\|_2.$$

Hence, it follows that

$$\|f_{t+1} - f^*\|_2 \leq \kappa \|f_t - f^*\|_2 + \eta \|\xi_t\|_2.$$

A.10. Proof of Proposition A.6

The proposition is a corollary of Lemma A.5. For the underlying boosting setting, we have $V(f) = \frac{1}{2}\|f - y\|_2^2$. Hence, $\mu = L = 1$. For $P(f) = \gamma I + A(f)$, we have $m = \gamma$ and $M = 1 + \gamma$. Condition $(f - f^*)^\top P(f) \nabla V(f) \geq m(f - f^*)^\top \nabla V(f)$ is equivalent to

$$(f - f^*)^\top P(f)(f - f^*) \geq m\|f - f^*\|_2^2$$

which holds as $MI \prec P(f)$.

B. Supplementary for Numerical Results

B.1. Information About Datasets

California Housing This dataset, from the StatLib repository, contains information about California districts and is used to predict the median house value. It includes data on housing characteristics, population, income, and geographic location, making it useful for regression tasks and geospatial analysis.

Diabetes Sourced from the UCI Machine Learning Repository, the diabetes dataset focuses on predicting disease progression one year after baseline measurements. It includes personal and medical indicators such as age, BMI, blood pressure, and blood serum levels, and is commonly used for regression modeling in healthcare studies.

Adult (Census Income) Also from the UCI Machine Learning Repository, the Adult dataset aims to classify whether an individual earns more than \$50K per year based on census data. It incorporates demographic and employment-related attributes, making it suitable for binary classification and regression tasks and studies on fairness and social analytics. In our study, the prediction target is defined to be the sum `education-num` (a numeric encoding of the categorical education feature) and `hours-per-week` (the number of hours an individual works per week).

German Credit This dataset, available from the UCI Machine Learning Repository, is used to predict creditworthiness, labeling individuals as having good or bad credit risk. It includes financial, personal, and loan-related information, providing a standard benchmark for classification and credit scoring problems. In our study, the prediction target is `CreditAmount`, an attribute representing the amount of credit (loan) requested by the individual.

Communities and Crime Sourced from the UCI Machine Learning Repository, the Communities and Crime dataset combines socio-economic, law enforcement, and crime rate statistics for US communities. It is typically used to predict violent crime rates based on community-level indicators, making it valuable for regression analysis and policy research. The prediction target is `ViolentCrimesPerPop`, which represents the violent crime rate per capita in a community.